RESEARCH MEMORANDUM

AN EXPERIMENTAL INVESTIGATION OF TWO INTERNAL-COMPRESSION AIR-INLET DESIGNS WHICH USE FLUID BOUNDARIES AS A MEANS OF SUPERSONIC COMPRESSION

By Robert R. Howell and Charles D. Trescot, Jr.

Langley Aeronautical Laboratory
Langley Field, Va.

NATIONAL ADVISORY COMMITTEE
FOR AERONAUTICS

WASHINGTON

August 14, 1958

NACA RM L58F06

NATIONAL ADVISORY COMMITTEE FOR AERONAUTICS

RESEARCH MEMORANDUM

AN EXPERIMENTAL INVESTIGATION OF TWO INTERNAL-COMPRESSION AIR-INLET DESIGNS WHICH USE FLUID BOUNDARIES AS A MEANS OF SUPERSONIC COMPRESSION*

By Robert R. Howell and Charles D. Trescot, Jr.

SUMMARY

A limited investigation of the internal-flow characteristics of two novel designs of internal-compression air inlets has been made in the Langley 9- by 12-inch supersonic blowdown tunnel at Mach numbers of 1.96 and 2.55. The tests were made at an angle of attack of 0° and a Reynolds number of approximately 6.7×10^6 per foot. The results of the tests show that a longitudinally slotted contracting channel and the effective contracting channel formed by the natural thickening of the boundary layer in a confined channel can be used to obtain pressure recoveries up to at least 0.90 of free-stream total pressure at a Mach number of 1.96 and 0.81 of free-stream total pressure at a Mach number of 2.55, provided large portions of the captured flow are bypassed. Such compression surfaces will also afford a range of stable and uniform flow near the peak pressure recovery value.

Additional research is needed to optimumize these designs and to establish the drag due to the bypassed flow and the performance characteristics at off-design flight conditions.

INTRODUCTION

The propulsive efficiency of air-breathing engines and, hence, the overall performance of jet-propelled aircraft is largely dependent upon the characteristics of the air flow to the engine. Included in the parameters which determine the engine air-flow characteristics are total-pressure recovery and flow stability and uniformity over the duct cross section at the engine inlet. The ideal flow characteristics, of course, correspond to a recovery of 100 percent stagnation pressure and, hence, uniform and steady velocity across the duct. As the speed of aircraft

*Title, Unclassified.

increases from Mach numbers of about 2.0 to much greater values, it becomes increasingly difficult to even approach these ideal engine airflow characteristics while satisfying the engine with its required rate flow of air which varies with Mach number and altitude. Variable geometry has been incorporated into some supersonic inlet designs in order that the large spillage drag and losses in pressure recovery resulting from inlet-engine mismatching can be avoided. (See, for example, refs. 1 to 3.) Although this required addition to the inlet design has generally made supersonic flight of air-breathing engines more efficient, there is still much to be desired in the internal-flow characteristics of supersonic air-intake systems.

The important gains in propulsion performance of aircraft that can result from improving the design of air-intake systems to be used at supersonic speeds warrant the exploration of new air-inlet design approaches which have possible merit. Two novel devices for obtaining supersonic compression are studied in the present investigation. One of the devices is a compression surface which may be described as an internally contracting longitudinally slotted surface; the other device may be described as the effective contracting surface provided by the internal boundary-layer growth under the large adverse pressure gradient present in short supersonic diffusers. In both cases, large quantities of the captured air flow were bypassed. The total-pressure recovery and its uniformity were measured at an assumed engine compressor face. The range of weight flow over which stable flow could be obtained was determined. Each design was tested in the Langley 9- by 12-inch supersonic blowdown tunnel near its design Mach number of 1.96, 2.06, or 2.50.

SYMBOLS

A	area
g	acceleration of gravity
M	Mach number
p	static pressure
p_t	total pressure at engine compressor face
$p_{t,\infty}$	free-stream total pressure

[redacted]

$\frac{\overline{p_t}}{p_{t,\infty}}$ average total-pressure ratio weighted with respect to local weight flow, $\frac{\int_A \left(\frac{g\rho V}{g\rho_\infty V_\infty}\right)\left(\frac{p_t}{p_{t,\infty}}\right) dA}{\int_A \left(\frac{g\rho V}{g\rho_\infty V_\infty}\right) dA}$

r radius

V velocity

w weight flow, lb/sec

$\frac{w_e}{w_c}$ engine weight-flow ratio

x longitudinal distance

η_{KE} kinetic energy efficiency (ref. 7)

ρ mass density, slugs/cu ft

Subscripts:

b bypass

c capture

des design

e engine

max maximum

∞ free stream

DESIGN CONSIDERATIONS

Design 1

The first air-inlet design utilized a longitudinally slotted internal-compression surface as a means of supersonic diffusion (fig. 1). The basic design is similar to the design of reference 4 in that spilling

flow through the supersonic diffuser walls allows supersonic flow in diffusers which have geometric contraction ratios equal to or greater than the theoretical maximum. Furthermore, this spilling allows the diffuser system to operate over a range of Mach numbers and at a higher pressure recovery as a result of flow removal ahead of the subsonic diffuser. The use of longitudinal slots was chosen rather than the circular holes used for the models in references 4 and 5 because it was felt that the slots could be designed to afford a more stable flow with less loss to the bypassed flow. For this design, the inlet shroud was sized relative to the throat such as to entrain a full free-stream tube ($w_e/w_c = 1.0$) at a Mach number of about 1.96. The lower Mach number for entrainment of a full-stream tube is determined by the maximum choking area of the bypass system, inasmuch as the difference between the maximum flow through the inlet throat and that captured by the shroud must be bypassed. (For this case, the lower design Mach number was about 1.5.) The upper operational Mach number limit for such a design is that Mach number where the airflow rate to the engine no longer satisfies the engine requirements or additional thrust from the engine can not be obtained.

The internal-compression surface and subsonic diffuser were designed by using one-dimensional flow relations and by using the arbitrarily chosen longitudinal Mach number distribution shown in figure 2. The rate of Mach number decrease in the supersonic diffuser, although probably far from optimum, was chosen in order to keep the overall system short and light. The ratio of inlet capture area to throat area was 1.64, which is the ideal area ratio for $M_\infty = 1.96$.

The bypass slots were designed to accommodate a weight flow equal to the difference in weight flow captured and that passable through the inlet throat at a Mach number of 1.5. The annular bypass exit was similarly sized. The rate at which the mass was removed, with distance along the slotted portion of the diffuser (fig. 3), was again an arbitrary choice. The primary objective was to remove the mass gradually and thereby avoid strong waves in the supersonic diffuser. The width of the slot openings at any point was governed by this distribution of flow removal. The slot width was calculated by assuming that one-eighth of the total flow to be bypassed at any point along the slot must pass through the slot perpendicular to the compression surface and at sonic velocity. The gradual decay of mass removed at the downstream end of the slots, in addition to allowing a smooth transition in flow removal rate, also provided a tapered slot which, it was believed, would be beneficial in achieving a range of engine weight-flow rates that would not be subject to instability.

The bypassed flow was channeled to the annular bypass in "U-shaped" channels. Each of the eight slots emptied into individual channels. The cross-sectional area of each channel at any longitudinal point was determined by integrating the curve for the desired bypass weight-flow removal

normal to the slot opening at each station from the forward end of the slot rearward to the desired station and then computing the area required to pass this total weight flow longitudinally if losses are assumed equal to those of a stream normal shock.

The design ordinates and pertinent dimensions for design 1 are presented in table I and figure 1.

Design 2

The second inlet was designed to utilize the natural growth of the internal boundary layer as a means of supersonic compression. It is known that at supersonic speeds the shock wave that stands ahead of forward-facing steps or subsonic air inlets is not a single wave at the surface but rather is a multiple wave as pictured in sketch A. In reference 6, for example, it is shown that for a fuselage side inlet the boundary layer separates ahead of the inlet and forms an effective wedge, as indicated in the sketch. The pressure recovery through the multiple shock wave is higher than that through a normal shock. Furthermore, for inlet weight-flow ratios of the order of 0.6, a major portion of the separated boundary layer sweeps around the sides of the inlet as a result of lateral pressure gradients.

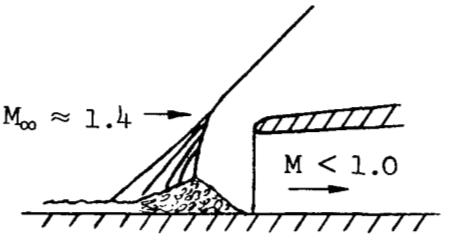

Sketch A

In the case of an axissymmetric open-nose inlet, the compression wave is a normal shock. (See sketch B.) Inasmuch as there is no shock—boundary-layer interaction, the only additional losses to the internal flow other than the normal shock loss are those associated with the subsonic diffuser.

Now if a cylinder were adjusted around the nose inlet to form a cowl or shroud, the compression wave might be expected to interact with the boundary layer on the inner surface of the cylinder in a manner similar to the interaction of the compression wave ahead

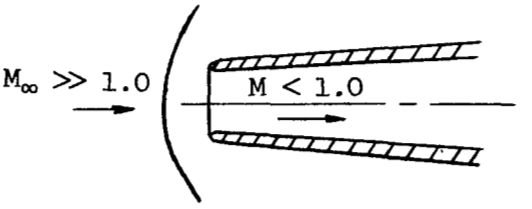

Sketch B

of the subsonic fuselage side inlet with the fuselage boundary layer (sketch C). This shock interaction should afford higher than normal shock pressure recovery, provided no separated flow enters the inlet throat. It would appear that the total height of the separated flow would depend, to a large extent, on the amount of flow allowed to bypass. This bypass flow rate, of course, depends on the weight flow allowed through the subsonic diffuser, on the bypass losses, and on the exit area. It is believed that a radial pressure gradient would exist for the described case which would tend to prevent the separated boundary layer from entering the subsonic diffuser, provided some bypassing is allowed at all times.

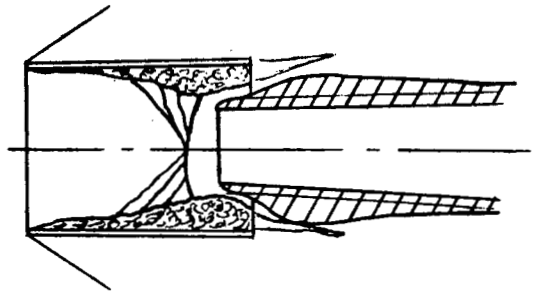

Sketch C

A configuration such as the one shown in sketch C might be expected to have flow characteristics similar to a fixed convergent-divergent diffuser and, hence, be unstable near its peak pressure recovery value. In order to increase the probability that some range of stable flow could be achieved, the inner surface of the shrouds tested was made to diverge conically from a point upstream of the subsonic diffuser inlet (figs. 4 and 5). The subsonic diffuser for this design was conical and had a divergence angle of 2.65° (fig. 4).

If stable flow could be attained for a usable range of engine weight-flow rate, it appeared that this approach to obtaining efficient supersonic compression might be practical. Accordingly, two "boundary-layer" compression inlets were designed. The primary difference between the two was a difference in contraction ratio. One inlet was designed to entrain a full-stream tube at $M_\infty = 2.06$ with a total-pressure ratio of 0.92 assumed at the subsonic diffuser inlet. The other inlet was designed to capture a full free-stream tube at a Mach number of 2.5 if a total-pressure ratio of 0.80 is assumed. The difference between the flow captured and that passed through the throat at design conditions was to be bypassed for both configurations. The bypass area was adjustable from fully closed to an open area equal to 2.61 square inches. A sketch showing pertinent dimensions for the cowls is presented in figure 5.

INSTRUMENTATION AND TESTS

A rake of 16 total and 3 static tubes was used to determine the engine weight-flow ratio, mean total-pressure ratio, and duct pressure profiles at an assumed compressor inlet station (fig. 6). This rake was used for all models. The pressures were recorded on flight-type quick-response pressure-recording instruments.

A rapid-response pressure pickup installed in the subsonic diffuser wall (figs. 1 and 4) was used to indicate the onset of unstable flow and buzz (oscillating flow). The output of this pickup was recorded on an oscillograph and monitored on an oscilloscope. As a result of an inability to check calibrations of the pickup before and after tests, the apprent magnitude of pressure oscillations was not considered accurate; hence, the pickup was used to denote unstable flow and buzz only.

Longitudinal static-pressure distributions were measured for the longitudinally slotted diffuser configuration (design 1) only. The location of these orifices is indicated in figure 1.

A limited attempt was made to measure the total-pressure recovery of the bypassed flow for design 1. The measurements, unfortunately, did not prove to be complete enough to give bypass drag information and consequently are not presented.

For some of the tests of design 2 (boundary-layer compression inlet), roughness particles and boundary-layer trip wires were used on the inner surface of the cowl or shroud to insure the existence of a thick turbulent boundary layer. The roughness particles used were from 0.012 to 0.018 inch in diameter and the trip wires were 0.021 inch in diameter; the location of each is indicated in figure 5.

The models were mounted on the tunnel center line at an angle of attack of 0°. The testing procedure was to preset the bypass area and control the weight flow through the subsonic diffuser with a remotely actuated exit plug. Data were taken for a number of "engine weight-flow rates" at each bypass area setting. A variation in engine weight-flow rate necessarily corresponds to a variation in bypass flow rate, inasmuch as the capture area always flows full. A shadowgraph system was used to insure that the cowl flowed full for all data points taken.

The tests were conducted in the Langley 9- by 12-inch supersonic blowdown tunnel at Mach numbers of 1.96 and 2.55. The corresponding nominal Reynolds numbers per foot were 6.8×10^6 and 6.6×10^6, and stagnation pressures were 25 and 32.2 pounds per square inch absolute,

respectively. In this investigation, data were obtained for each configuration at near design Mach number only.

[redacted]

Design 1

The average total-pressure ratio as a function of engine weight-flow ratio for the longitudinally slotted inlet, as tested at a Mach number of 1.96, is presented as figure 7 for various bypass exit areas. The weight-flow ratios where instability and buzz were observed are indicated. Inasmuch as that portion of the weight-flow range characterized by buzz is not generally considered acceptable, the following discussion is restricted to stable flow conditions only. It might be of interest, however, to note that two types of buzz were observed during the test. The more conventional low-frequency buzz was observed at the low weight-flow ratios where the terminal shock was upstream of the diffuser throat. At the high weight-flow ratios, when the shock stood in the subsonic diffuser, a higher frequency, lower amplitude buzz or oscillation was observed. It is not clear from these present data whether this high-frequency buzz originates from the terminal shock in the diffuser or from some phenomena in the bypass system.

It is indicated in figure 7 that the peak pressure ratio obtained with this configuration at a Mach number of 1.96 was about 0.90. The inability to achieve weight-flow ratios greater than about 0.8 is attributed to the fact that the bypass exit area was not remotely controlled. The minimum bypass area allowed, therefore, was determined by inlet starting requirements. For exit plug settings larger than those required for the data presented, obvious errors in pressure measurements at the compressor face, presumably associated with the unsteady flow present, prevented accurate weight-flow calculations; therefore, these data are not presented.

Typical total-pressure distributions over the duct of the assumed compressor face station are presented in figure 8(a). Here the local values of $p_t/p_{t,\infty}$ are plotted against $(r/r_{max})^2$. For the cases where near maximum average pressure ratio was obtained, it is seen that the total-pressure distribution over the duct was fairly flat. Generally, the departures from uniformity were about ±2 percent. Only for cases near the maximum weight-flow ratios where the terminal shock stands in the subsonic diffuser was there any large distortion. The tendency for the pressure ratio to drop off toward the center of the duct (where $(r/r_{max})^2 = 0$) probably indicates the presence of a normal shock segment in the compression wave pattern or vortex core, or both, on the axis of the diffuser.

[redacted]

The variation in weight-flow ratio for peak pressure ratio with changes in bypass exit area are presented as figure 9. The width of the hatched envelope curve indicates the possible experimental error band and corresponds to the maximum total-pressure ratios afforded by this inlet for the usable engine weight-flow range at the test Mach number of 1.96. It is indicated that, for this design, a considerable change in geometric bypass area was necessary before an appreciable shift in the weight flow for peak pressure ratio was obtained. It is apparent from this result that there was either a large change in the losses in the bypass flow with changes in bypass area or the choking area of the bypass system is not always located at the geometric exit area. It appears, however, that a range of engine weight-flow ratio ($0.55 \leqq w_e/w_c \leqq 0.8$) at average pressure ratios between 0.8 and 0.9 can be obtained with this design at Mach numbers near 2.0 through the use of a variable bypass area control. It should be noted that this configuration is not considered to be optimum from any standpoint and most probably could be improved by a number of changes. For example, the longitudinal static-pressure distributions for this configuration (fig. 10 is typical) indicate that for maximum total-pressure ratio the static-pressure rise is 95 percent complete at the end of the slotted supersonic diffuser. The long subsonic diffuser increases the static recovery only about 5 percent. It would appear reasonable to expect that a gain in both mean pressure ratio and stable weight-flow ratio range could be obtained by increasing the length of the slotted supersonic portion of the diffuser system. There would, of course, be a corresponding reduction in bypass slot width and depth in order to maintain, if desired, the present bypass flow rate. From the standpoint of the designer it would probably be advantageous to reduce the subsonic diffuser length, since the diffuser contributes little in pressure ratio, and to change the duct diameter to its desired size by making use of the reduction of duct cross-sectional area caused by the presence of the spinner-shaped accessory housing that normally protrudes as a center body ahead of the engine. In addition to these possible changes, there is also the possibility of changes in bypass slot and ducting design in order to obtain a more optimum supersonic diffusion.

Design 2 (M_{des} = 2.06)

The variation of mean total-pressure ratio with engine weight-flow ratio for the Mach number 2.06 design "boundary-layer compression inlet" is presented in figure 11 for various bypass areas as obtained at a Mach number of 1.96. It is shown that the peak pressure ratio for this configuration (M = 1.96) was about 0.90. This result is comparable to the results obtained with the slotted diffuser configuration and other more common configurations such as conical spike inlets and is somewhat

surprising inasmuch as the ratio was obtained without a physical compression surface. The variation in pressure ratio with weight-flow ratio for this case was dependent upon the boundary-layer characteristics inside the cowl or shroud. As indicated in the figure, only slightly better than normal shock recovery was obtained with the inner surface of the cowl smooth. With large roughness particles fixed, as indicated in figure 5, much higher pressure ratios were obtained. The reason for this result is not clear from the data obtained in the present, limited tests. The buzz points which bracket the range of stable flow for some of the cases presented indicate the onset of the two types of buzz noted earlier in this section. The uniformity of total pressure over the duct cross section at the assumed compressor station was as good for this inlet as for the slotted inlet. (Compare figs. 8(a) and 8(b).)

The variation in weight-flow ratio from peak pressure ratio with variation in bypass area is shown in figure 12. It should be noted that the hatched wide envelope curve is much flatter for this design than for the slotted diffuser design (fig. 9). Furthermore, the variation in weight-flow ratio with variation in bypass area is much more systematic than in the slotted diffuser case. As was mentioned previously, this difference in flow phenomena between the two designs may possibly be attributed to the bypass loss difference between the two cases and may, therefore, be subject to change with changes in the slotted diffuser design.

It should be noted that near design Mach number ($M = 2.06$) this inlet design principle will provide uniform and stable airflow over a range of weight-flow ratio ($0.55 \leqq w_e/w_c \leqq 0.75$) at pressure ratios between 0.86 and 0.90. Here, again, the maximum value of w_e/w_c could probably be increased by remotely controlling the bypass exit area.

Design 2 ($M_{des} = 2.50$)

The variation in total-pressure ratio with engine weight-flow ratio for two bypass area settings is presented in figure 13. These data were obtained from tests at a Mach number of 2.55. As indicated, the peak pressure ratio obtained was 0.81. The variation of pressure ratio with w_e/w_c greater than that for peak pressure ratio was similar to that obtained with the slotted diffuser inlet. This trend was not observed for the Mach number 2.06 design. The presence of boundary-layer trip wires (fig. 5) seemed to cause a reduction in pressure ratio for all weight-flow ratios except those near peak pressure-ratio value. This result is in contrast to the requirement of roughness in the Mach number 2.0 design case in order to obtain peak pressure ratios. At the smaller bypass area presented, a hysteresis loop of pressure recovery against weight-flow ratio is apparent which is a general characteristic of high-performance

internal-contracting inlet designs such as the ones tested here. This hysteresis loop is not necessarily of great importance, provided operation of the inlet is kept near the peak of pressure ratio curve.

It should be noted that even at a Mach number of 2.55 the total-pressure distribution at the compressor face station was fairly uniform (fig. 8(c)).

DISCUSSION OF RESULTS

By observation of a shadowgraph of the inlet during the tests, it was assured that the cowl flowed full at all times; hence, there is no drag associated with the entering flow. The drag, in this case, is associated entirely with the external cowl shape, which can be optimumized, and with the losses in bypassed flow, which should be amenable to control through proper design. Inasmuch as no acceptable bypass loss or drag measurements were obtained during these tests, a comparison of the present methods of supersonic compression with other methods can be made only on the basis of internal-flow characteristics. Figure 14 provides an insight into the relative potentialities of these present methods insofar as average pressure ratio is concerned. In this figure, the maximum average total-pressure ratio for each inlet configuration compared is shown plotted as a function of Mach number. It is indicated that the peak pressure ratio for the present designs is above that for fixed conical spike inlets and also above those of a translating spike inlet which was designed to alleviate pressure drag at Mach numbers of 2.5 and above by having zero lip camber (ref. 1). The present peak pressure ratios are indicated to fall below those of a translating spike inlet, designed for a Mach number of 3.0, which incorporates inlet lip camber and boundary-layer removal at the throat (ref. 3). The curves of constant kinetic-energy-efficiency levels (ref. 7) also shown in figure 14 indicate that the present inlet designs are fairly efficient insofar as pressure ratios are concerned. The range of stable uniform weight flow at high pressure ratios and at specific Mach numbers for the present cases is somewhat larger than those measured for the reference configurations. This feature should be significantly advantageous from an operational standpoint.

It is apparent that if the bypassed flow can be discharged without excessive loss and if the external cowl shape can be designed for low drag, the overall performance of the present air-inlet designs could be good. Additional research to provide information concerning both internal characteristics as well as drag due to bypassing flow for a range of Mach numbers and angles of attack over which such inlets are required to operate is needed prior to complete evaluation of these present supersonic inlet designs.

[redacted]

CONCLUDING REMARKS

A limited investigation of the internal-flow characteristics of two novel designs of internal-compression devices has been made in the Langley 9- by 12-inch supersonic blowdown tunnel at near the design Mach numbers of 1.96, 2.06, and 2.50. The results of this investigation showed that a longitudinally slotted contracting surface tested at $M = 1.96$ and the effective contracting surface resulting from the natural thickening of the boundary layer in a short confined channel tested at $M = 1.96$ and $M = 2.55$ can be used to obtain pressure recoveries up to at least 0.90 of free-stream total pressure at a Mach number of 1.96 and up to at least 0.81 of free-stream total pressure at a Mach number of 2.55. These recoveries were obtained while bypassing approximately 35 and 25 percent of the captured flow, respectively. The compression surfaces also afforded a range of stable and uniform flow near the peak pressure-ratio value.

Additional research is needed to optimumize these designs and to establish the drag due to the bypassed flow and the performance characteristics at off-design flight conditions.

Langley Aeronautical Laboratory,
National Advisory Committee for Aeronautics,
Langley Field, Va., May 26, 1958.

[redacted]

REFERENCES

1. Mossman, Emmet A., and Pfyl, Frank A.: An Experimental Investigation at Mach Numbers From 2.1 to 3.0 of Circular-Internal-Contraction Inlets With Translating Centerbodies. NACA RM A56G06, 1956.

2. Scherrer, Richard, and Cowen, Forrest E.: Preliminary Experimental Investigation of a Variable-Area, Variable-Internal-Contraction Air Inlet at Mach Numbers Between 1.42 and 2.44. NACA RM A55F23, 1955.

3. Connors, James F., Lovell, J. Calvin, and Wise, George A.: Effects of Internal-Area Distribution, Spike Translation, and Throat Boundary-Layer Control on Performance of a Double-Cone Axisymmetric Inlet at Mach Numbers from 3.0 to 2.0. NACA RM E57F03, 1957.

4. Evvard, John C., and Blakey, John W.: The Use of Perforated Inlets for Efficient Supersonic Diffusion. NACA TN 3767, 1957.

5. McLafferty, George: Tests of Perforated Convergent-Divergent Diffusers for Multi-Unit Ramjet Application. Rep. R-53133-19 (Contract NOa(s)-9661), Res. Dept., United Aircraft Corp., June 1950.

6. Bingham, Gene J.: Investigation at Transonic Speeds of Aerodynamic Characteristics of an Unswept Semielliptical Air Inlet in the Root of a 45° Sweptback Wing. NACA RM L55F22a, 1955.

7. Connors, James F., and Allen, John L.: Survey of Supersonic Inlets for High Mach Number Applications. NACA RM E58A20, 1958.

TABLE I.- DESIGN COORDINATES FOR SLOTS OF DESIGN 1

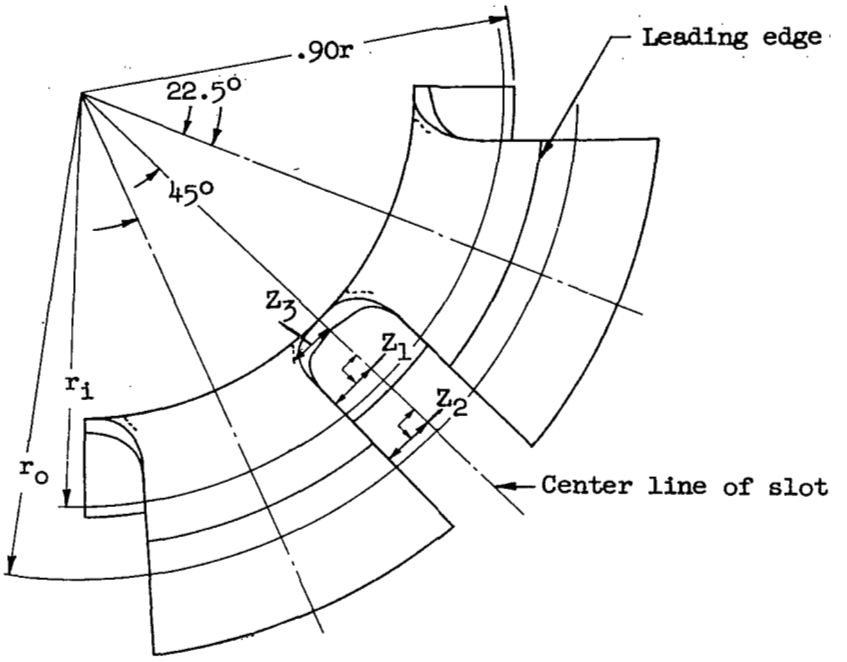

Z_1 and Z_2 perpendicular to center line of slot. Side walls beneath overhang parallel to center line of slot except where Z_3 is used.

Slot Coordinates					
Station	r_i	r_o	Z_1	Z_2	Z_3
0	0.961	0.961	0.125	0.125	
.2	.929	.950	.125	.127	
.4	.900	.959	.127	.131	
.6	.874	.976	.129	.134	
.8	.849	1.005	.129	.135	
1.0	.828	1.036	.130	.137	
1.2	.810	1.073	.130	.138	
1.4	.795	1.113	.127	.140	
1.6	.781	1.151	.121	.141	0.121
1.8	.771	1.189	.112	.145	.125
2.0	.761	1.223	.098	.147	.125
2.2	.755	1.273	.070	.150	.125
2.4	.755	1.298	.030	.167	.127
2.5			0	.226	.130
2.6		1.311		.285	.135
2.8		1.311		.353	.172
3.0		1.311		.431	.220
3.2		1.311		.510	.296

Design coordinates of subsonic diffuser		
Sta.	r_i	r_o
2.87	0.756	0.90
3.12	.757	.90
4.12	.765	1.10
5.12	.773	1.29
6.12	.798	1.30
7.12	.826	1.25
8.12	.873	1.25
9.12	.954	1.25
9.37	1.000	1.25

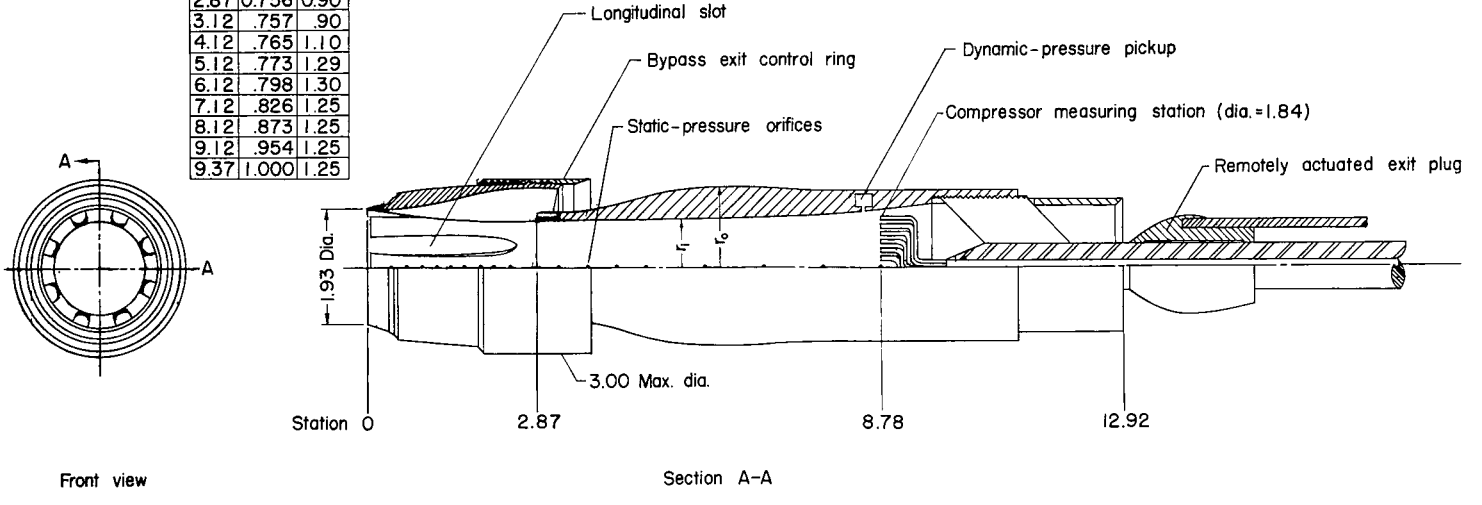

Figure 1.- Sketch showing details of slotted inlet design. All dimensions are in inches.

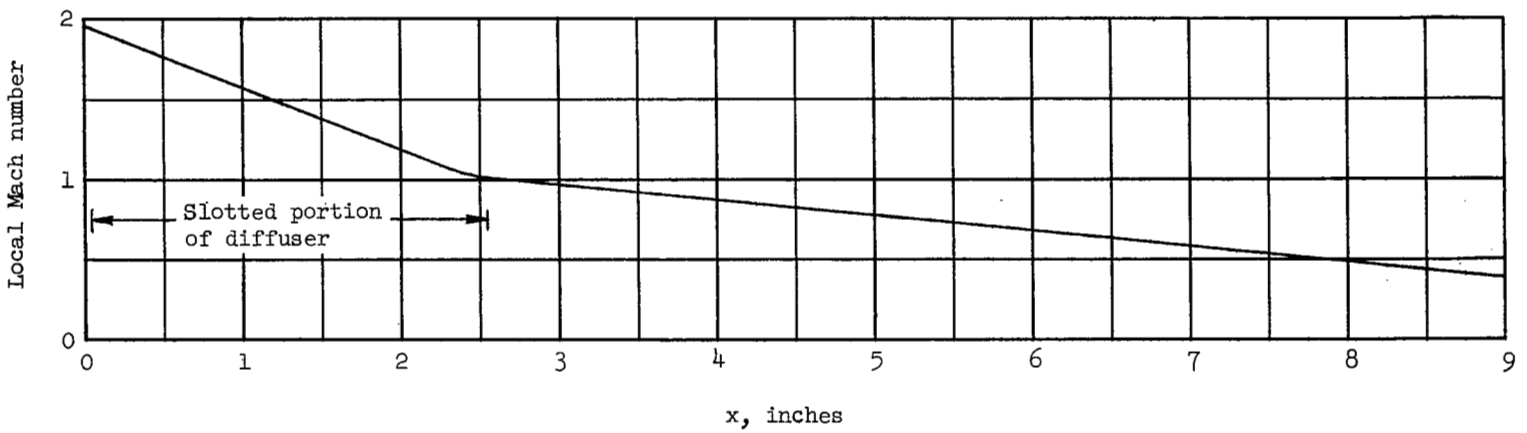

Figure 2.- Mach number distribution assumed for one-dimensional calculation of duct area development.

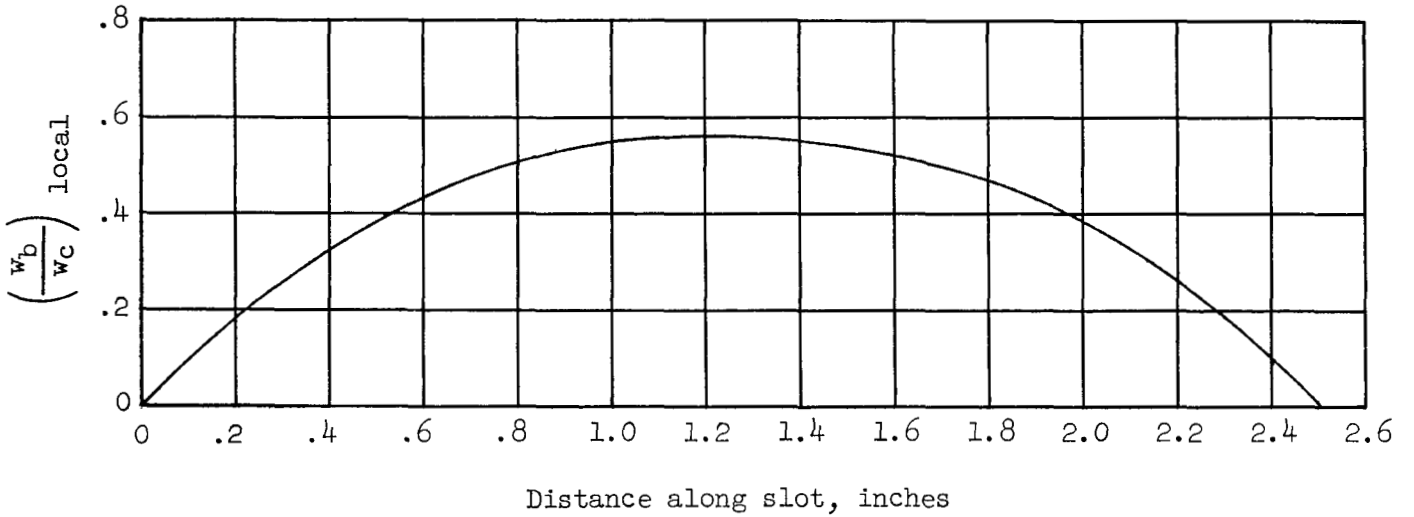

Figure 3.- Distribution of local flow removal used in calculating slot shape and bypass geometry.

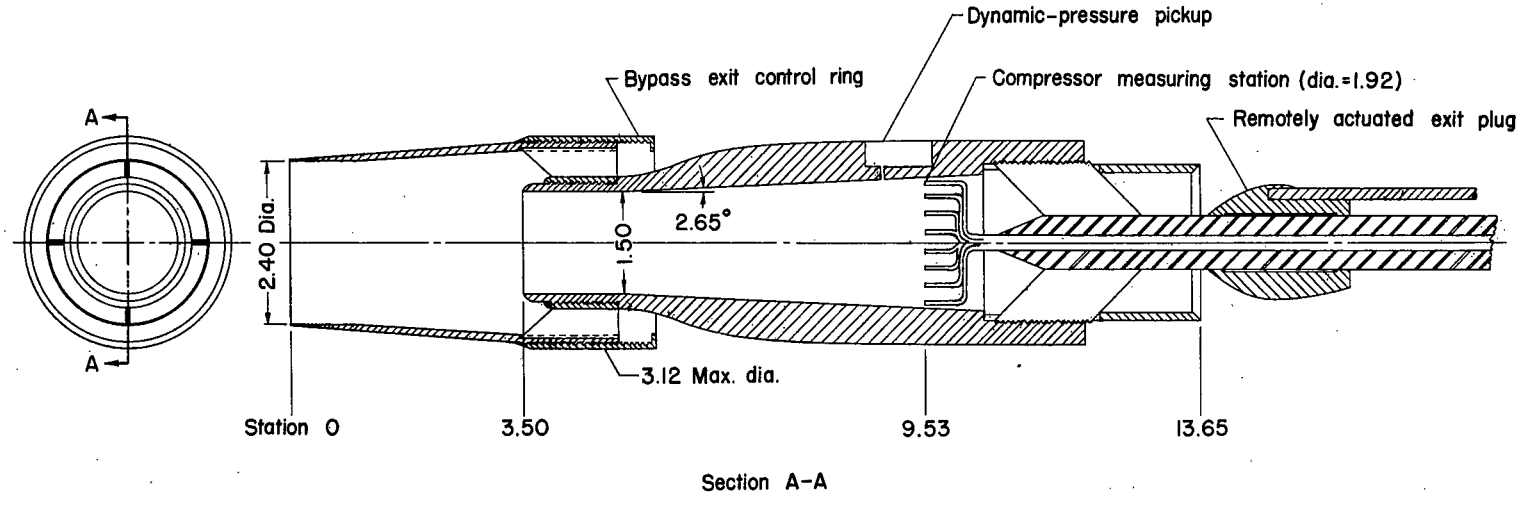

Figure 4.- Sketch showing details of boundary-layer compression inlet design. M_{des} = 2.5 shroud shown. All dimensions are in inches.

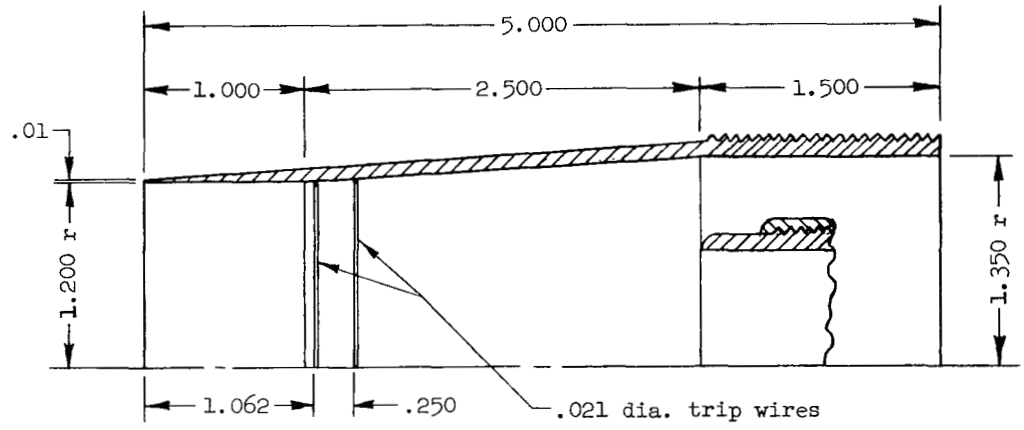

M_{des} = 2.50 inlet shroud

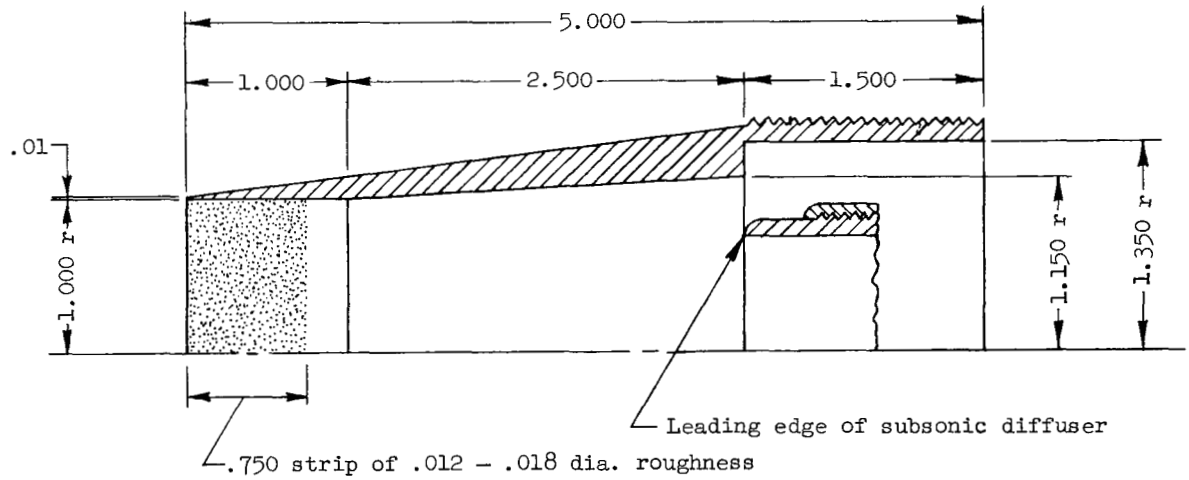

M_{des} = 2.06 inlet shroud

Figure 5.- Sketch showing design dimensions of M_{des} = 2.06 and M_{des} = 2.5 inlet shrouds for design 2. All dimensions are in inches.

[redacted]

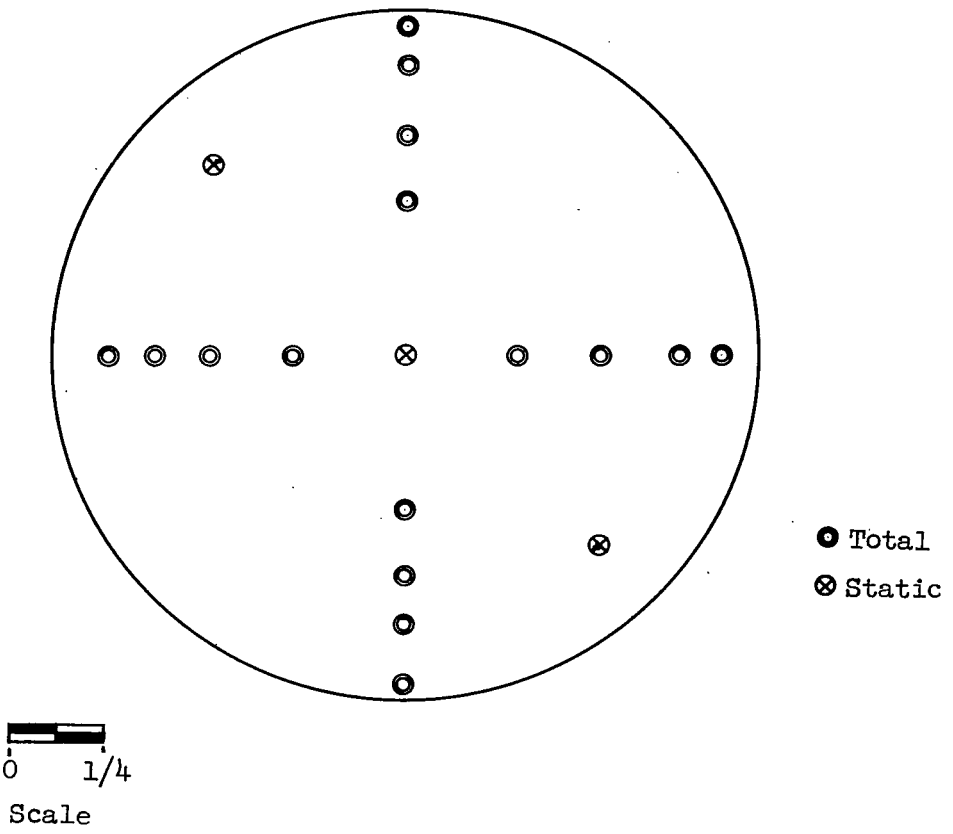

Figure 6.- Distribution of total- and static-pressure tubes at assumed engine compressor measuring station for slotted inlet and for boundary-layer compression inlets.

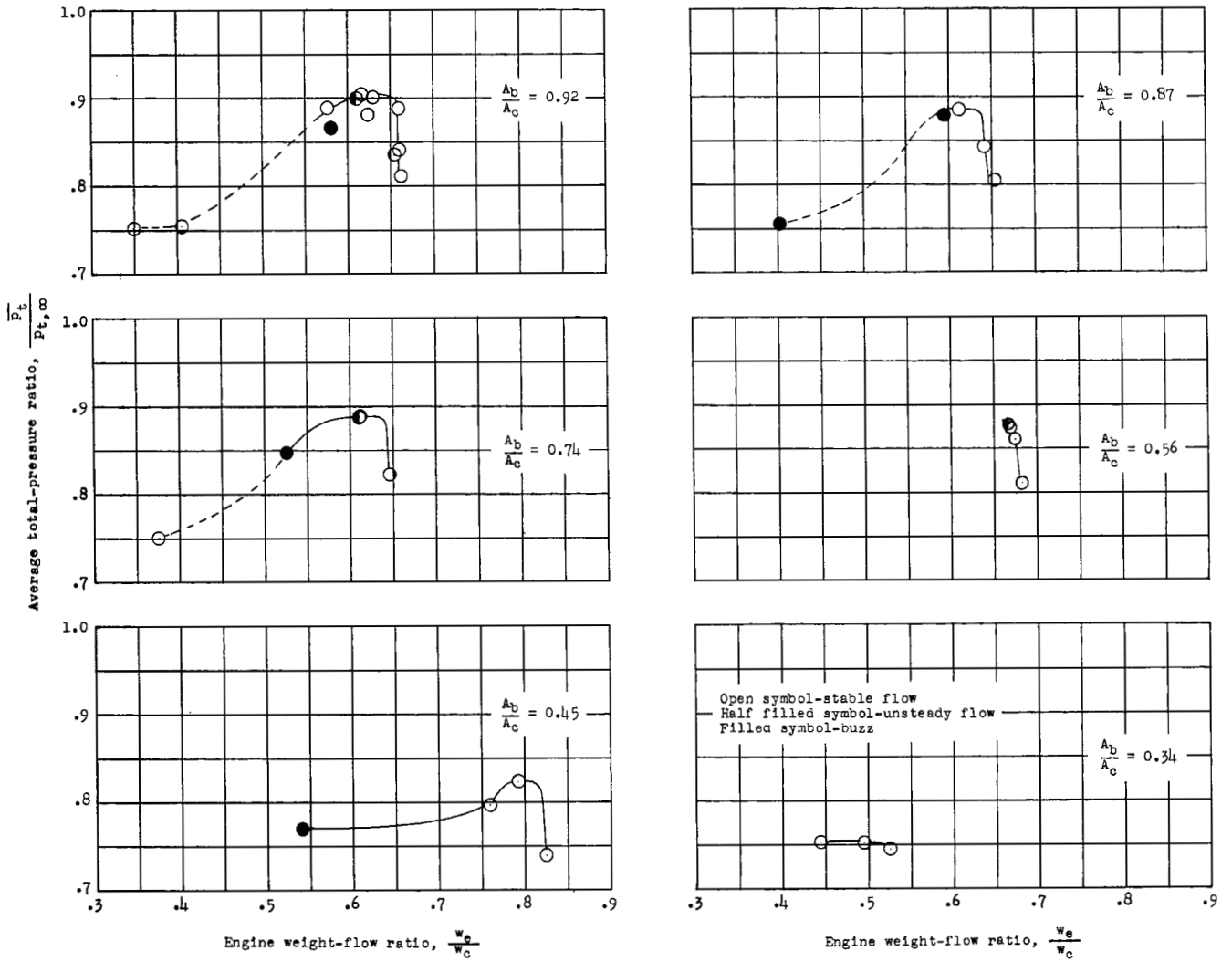

Figure 7.- Variation in mean total-pressure ratio with engine weight-flow ratio for various bypass exit-area settings. Slotted inlet. M_∞ = 1.96.

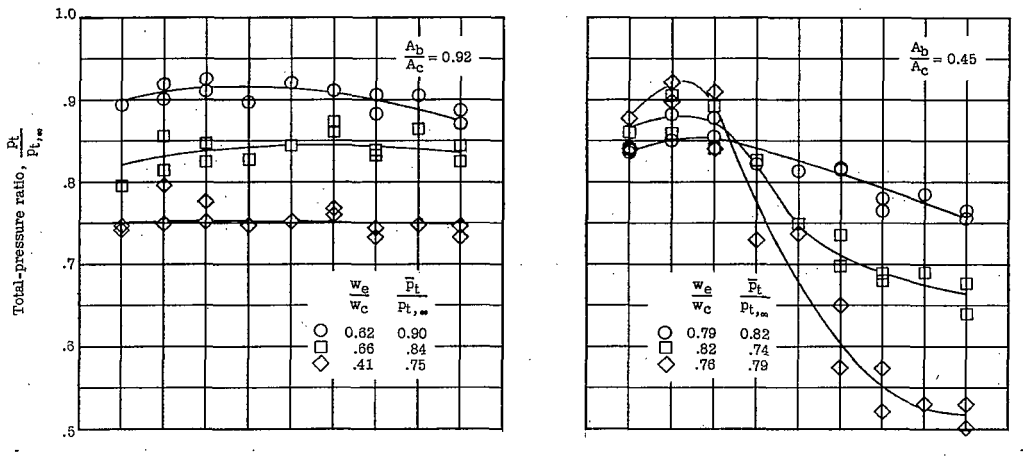

(a) Design 1 (M_{des} = 1.96).

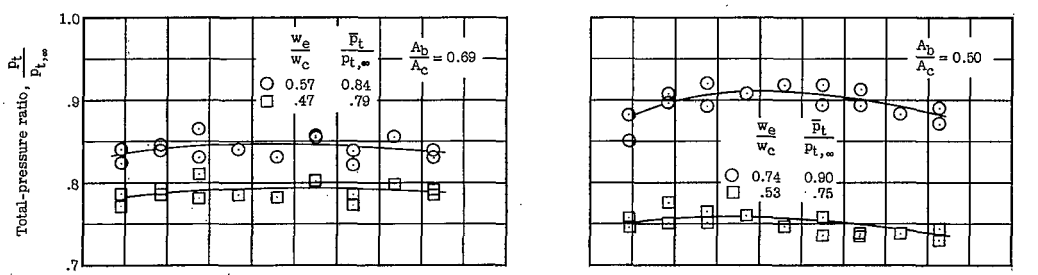

(b) Design 2 (M_{des} = 2.06).

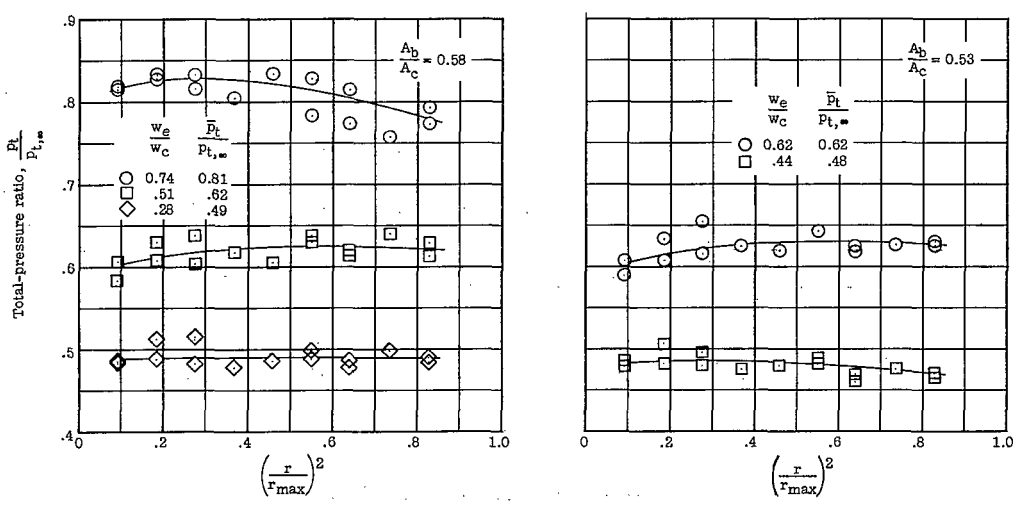

(c) Design 2 (M_{des} = 2.50).

Figure 8.- Typical distributions of total-pressure ratio over duct at assumed engine-inlet station.

[redacted]

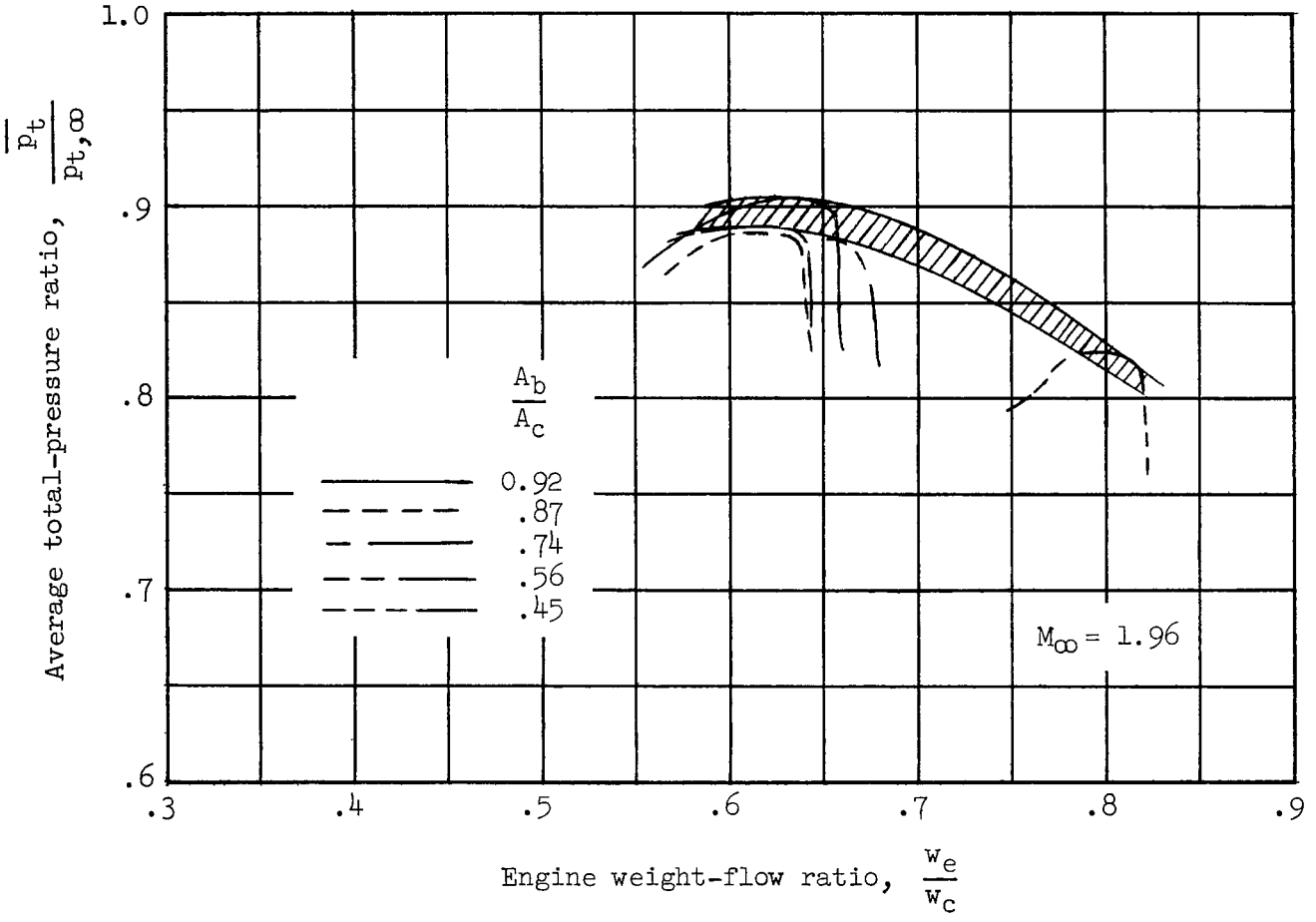

Figure 9.- Variation in engine weight-flow ratio for peak average pressure ratio with changes in bypass exit area for slotted inlet.

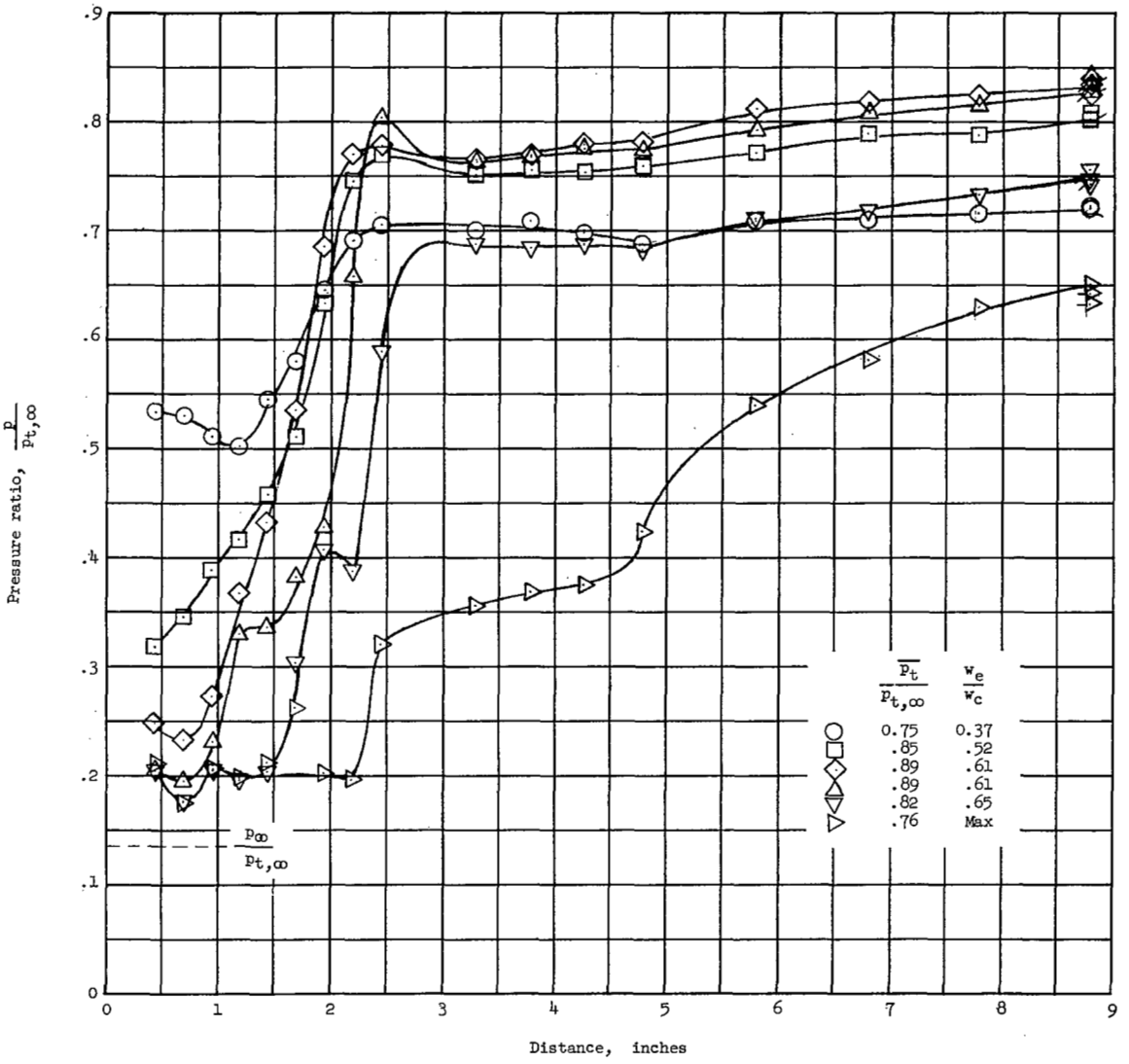

Figure 10.- Typical variations in longitudinal static-pressure distributions with changes in engine weight-flow ratio for the slotted inlet. Ticked symbols indicate pressures measured in rake plane. $M_\infty = 1.96$; $\frac{A_b}{A_c} = 0.74$.

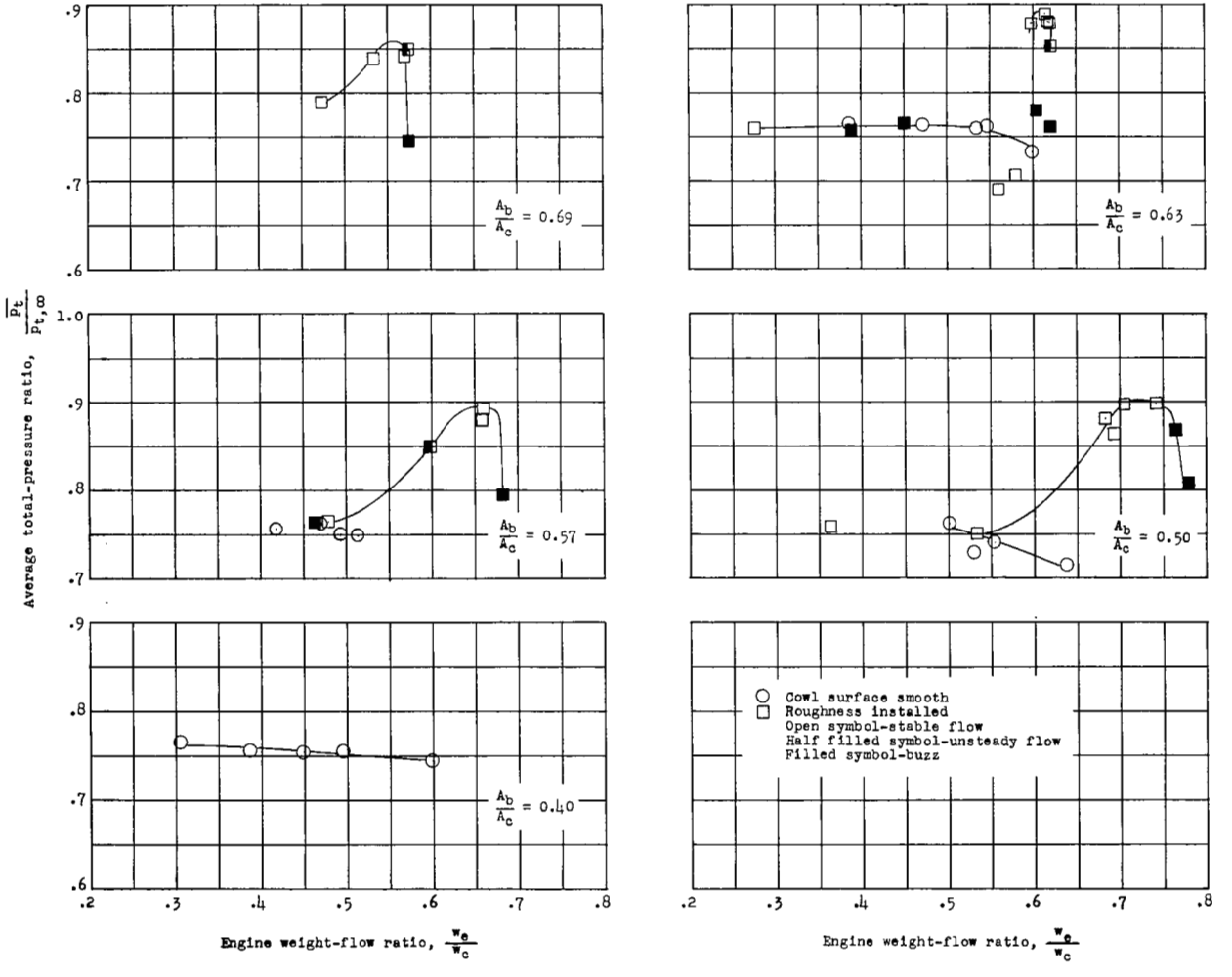

Figure 11.- Variation in mean total-pressure ratio with engine weight-flow ratio for various bypass exit-area settings. Boundary-layer compression inlet. M_{des} = 2.06; M_∞ = 1.96.

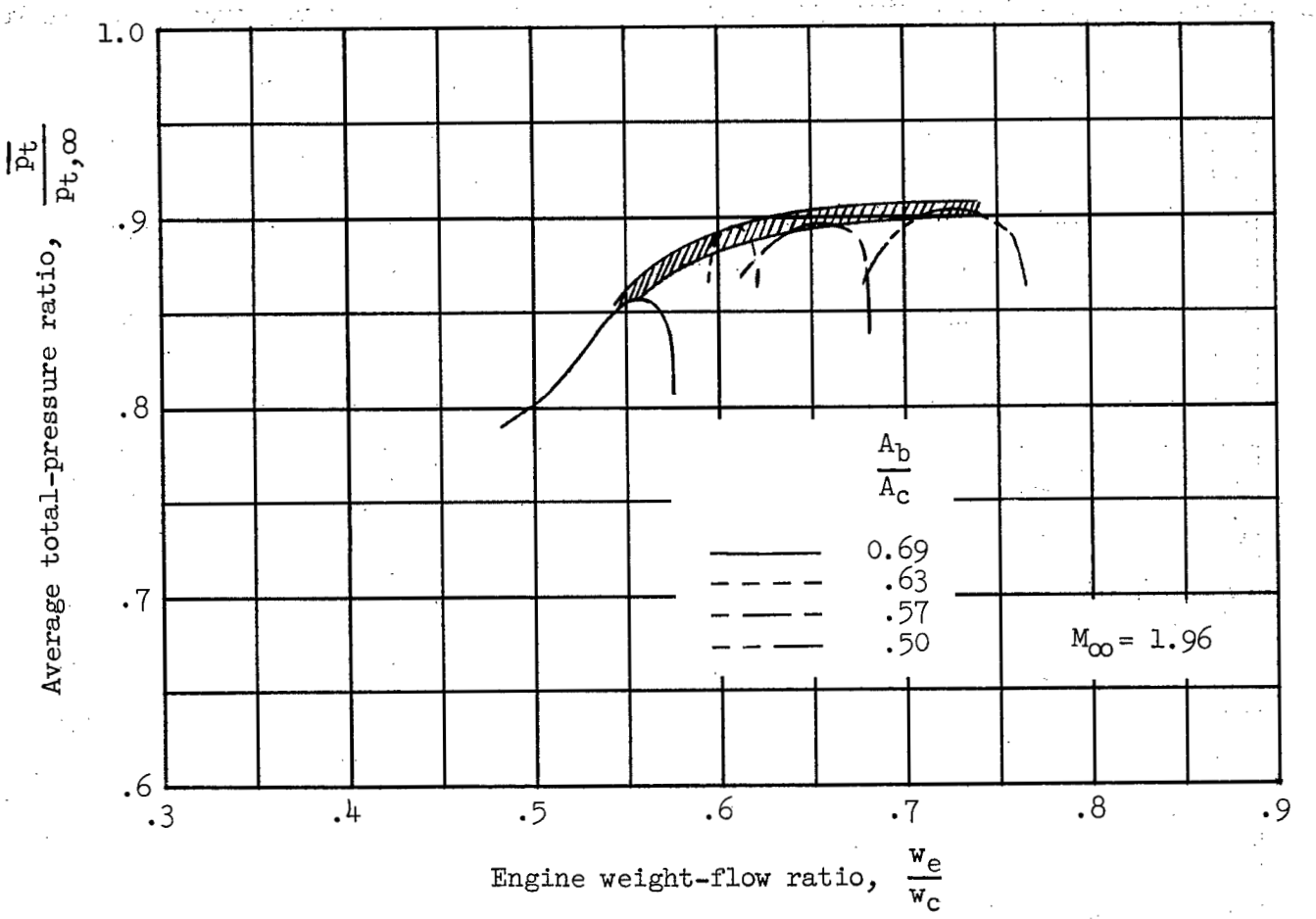

Figure 12.- Variation in engine weight-flow ratio for peak pressure ratio with changes in bypass exit area. Boundary-layer compression inlet. $M_{des} = 2.06$.

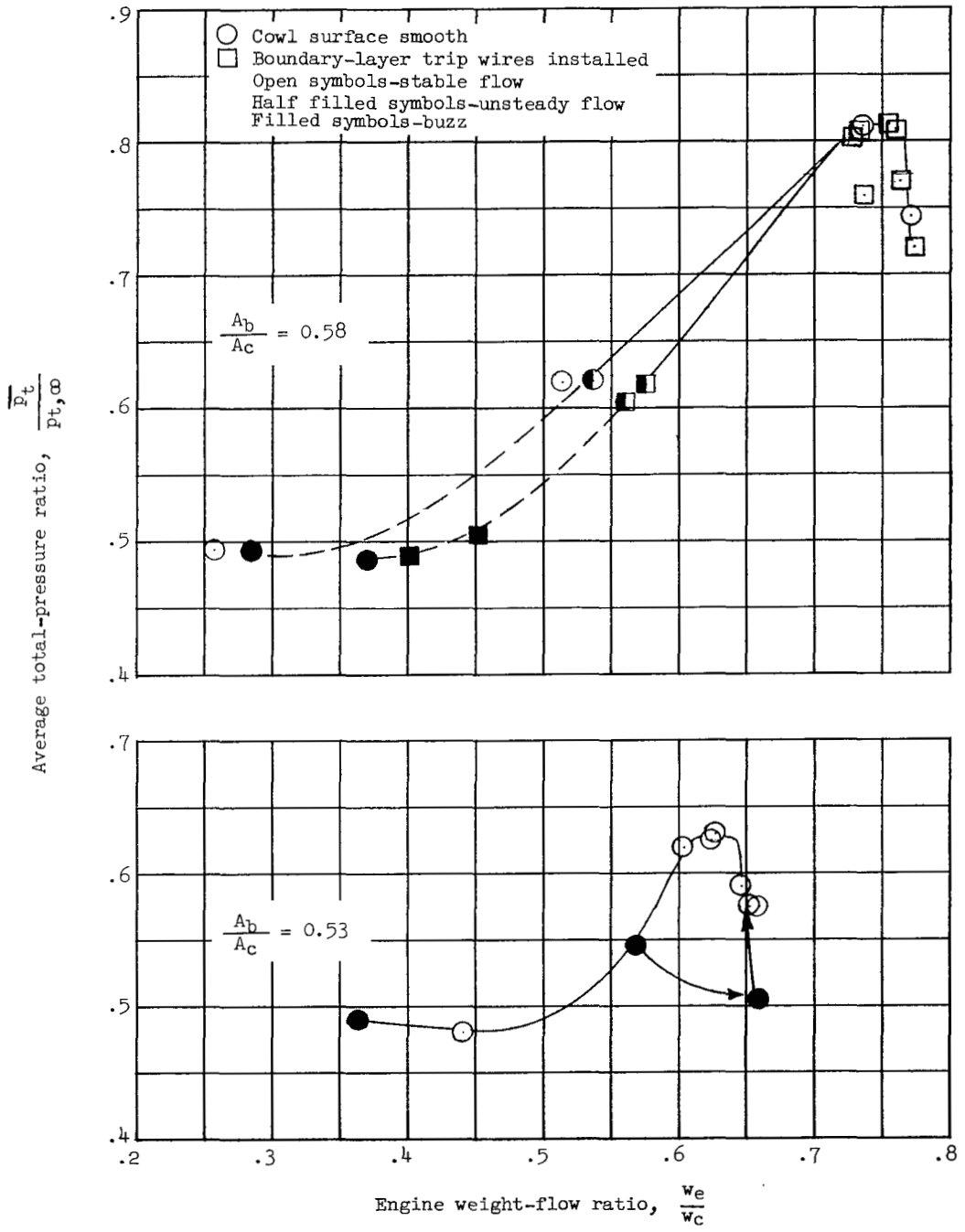

Figure 13.- Variation in mean total-pressure ratio with engine weight-flow ratio for two bypass exit-area settings. Boundary-layer compression inlet. M_{des} = 2.5; M_∞ = 2.55.

[redacted]

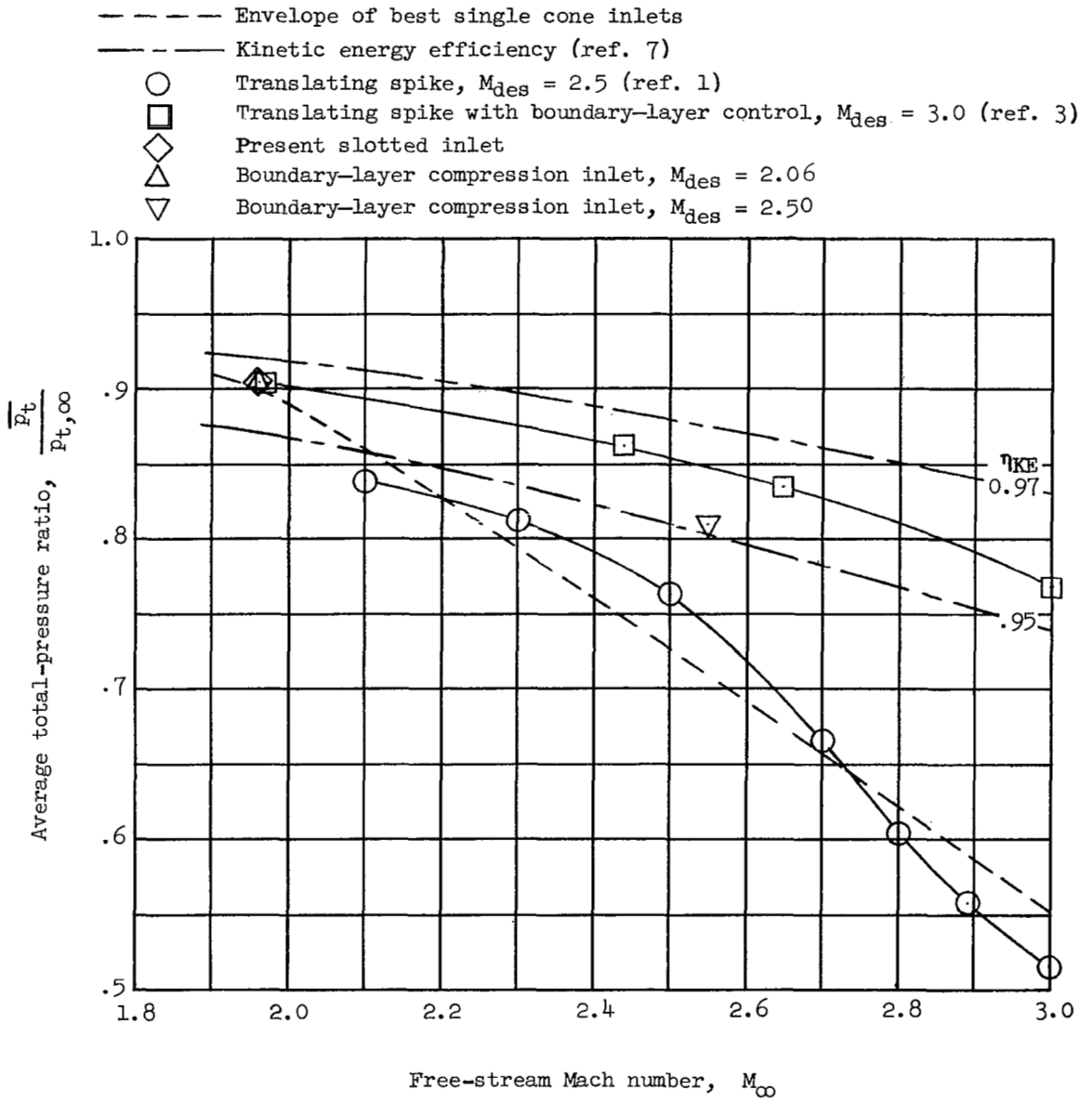

Figure 14.- Comparison of peak average total-pressure ratios of a number of good air inlets with those of the present designs.

NACA - Langley Field, Va.

NOTES: (1) Reynolds number is based on the diameter of a circle with the same area as that of the capture area of the inlet.

(2) The symbol * denotes the occurrence of buzz.

Report and facility	Description			Test parameters				Test data				Performance		Remarks
	Configuration	Number of oblique shocks	Type of boundary-layer control	Free-stream Mach number	Reynolds number × 10^{-6}	Angle of attack, deg	Angle of yaw, deg	Drag	Inlet-flow profile	Discharge-flow profile	Flow picture	Maximum total-pressure recovery	Mass-flow ratio	
Confid. RM L58F06 Langley 9" by 12" Supersonic Blowdown Tunnel	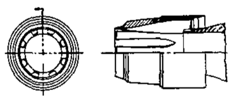			1.96	1.09	0	0			√		0.90	0.35-0.82*	
Confid. RM L58F06 Langley 9" by 12" Supersonic Blowdown Tunnel	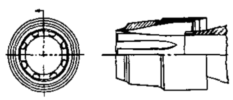			1.96	1.09	0	0			√		0.90	0.35-0.82*	
Confid. RM L58F06 Langley 9" by 12" Supersonic Blowdown Tunnel	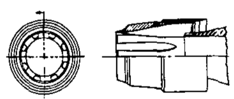			1.96	1.09	0	0			√		0.90	0.35-0.82*	
Confid. RM L58F06 Langley 9" by 12" Supersonic Blowdown Tunnel	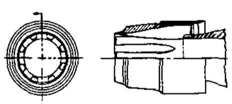			1.96	1.09	0	0			√		0.90	0.35-0.82*	

Bibliography

These strips are provided for the convenience of the reader and can be removed from this report to compile a bibliography of NACA inlet reports. This page is being added only to inlet reports and is on a trial basis.

NOTES: (1) Reynolds number is based on the diameter of a circle with the same area as that of the capture area of the inlet.

(2) The symbol * denotes the occurrence of buzz.

Report and facility	Description			Test parameters				Test data				Performance		Remarks
	Configuration	Number of oblique shocks	Type of boundary-layer control	Free-stream Mach number	Reynolds number $\times 10^{-6}$	Angle of attack, deg	Angle of yaw, deg	Drag	Inlet-flow profile	Discharge-flow profile	Flow picture	Maximum total-pressure recovery	Mass-flow ratio	
Confid. RM L58F06 Langley 9" by 12" Supersonic Blowdown Tunnel	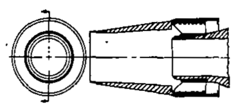			1.96	1.13	0	0			√		0.90	0.28-0.78*	
Confid. RM L58F06 Langley 9" by 12" Supersonic Blowdown Tunnel	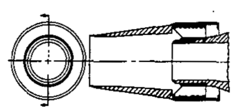			1.96	1.13	0	0			√		0.90	0.28-0.78*	
Confid. RM L58F06 Langley 9" by 12" Supersonic Blowdown Tunnel	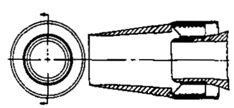			1.96	1.13	0	0			√		0.90	0.28-0.78*	
Confid. RM L58F06 Langley 9" by 12" Supersonic Blowdown Tunnel	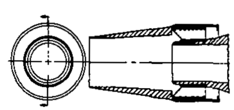			1.96	1.13	0	0			√		0.90	0.28-0.78*	

Bibliography

These strips are provided for the convenience of the reader and can be removed from this report to compile a bibliography of NACA inlet reports. This page is being added only to inlet reports and is on a trial basis.

[redacted]

NOTES: (1) Reynolds number is based on the diameter of a circle with the same area as that of the capture area of the inlet.

(2) The symbol * denotes the occurrence of buzz.

Report and facility	Description			Test parameters				Test data				Performance		Remarks
	Configuration	Number of oblique shocks	Type of boundary-layer control	Free-stream Mach number	Reynolds number $\times 10^{-6}$	Angle of attack, deg	Angle of yaw, deg	Drag	Inlet-flow profile	Discharge-flow profile	Flow picture	Maximum total-pressure recovery	Mass-flow ratio	
Confid. RM L58F06 Langley 9" by 12" Supersonic Blowdown Tunnel	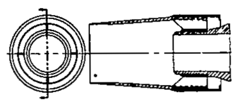			2.55	1.32	0	0			√		0.81	0.26-0.78*	
Confid. RM L58F06 Langley 9" by 12" Supersonic Blowdown Tunnel	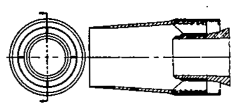			2.55	1.32	0	0			√		0.81	0.26-0.78*	
Confid. RM L58F06 Langley 9" by 12" Supersonic Blowdown Tunnel	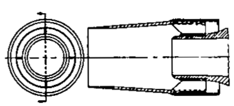			2.55	1.32	0	0			√		0.81	0.26-0.78*	
Confid. RM L58F06 Langley 9" by 12" Supersonic Blowdown Tunnel	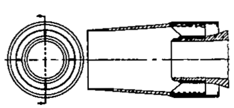			2.55	1.32	0	0			√		0.81	0.26-0.78*	

Bibliography

These strips are provided for the convenience of the reader and can be removed from this report to compile a bibliography of NACA inlet reports. This page is being added only to inlet reports and is on a trial basis.

[redacted]